

Mechanical properties of Si_3N_4 – graphene composites sintered by SPS method

Piotr Klimczyk¹, Lucyna Jaworska¹, Sławomir Cygan¹, Jerzy Morgiel², Łukasz Major², Andrzej Olszyna³

¹The Institute of Advanced Manufacturing Technology, ul. Wroclawska 37A, 30-011 Krakow, Poland

²Institute of Metallurgy and Materials Science, Polish Academy of Science, ul. W. Reymonta 25, 30-059 Krakow, Poland

³Warsaw University of Technology, Faculty of Materials Science and Engineering, ul. Wołoska 141, 02-507 Warsaw, Poland

E-mail: piotr.klimczyk@ios.krakow.pl

Received: 26.09.2017. Accepted in revised form: 29.12.2017.

© 2017 Instytut Odlewnictwa. All rights reserved.

DOI: 10.7356/ioid.2017.20

Abstract

Silicon nitride powder with a small addition of magnesium oxide and yttria stabilized tetragonal zirconia fine particles was used as a starting material. Multilayer graphene nanoplatelets were used as filler for silicon nitride based composites. Graphene content in the mixtures was 0–2 wt. %. The composites were obtained by the Spark Plasma Sintering method at 1650°C under 35 MPa of uniaxial pressure. Separation of the agglomerated graphene platelets in the matrix was observed for these materials. Insufficient dispersity of graphene slightly decreased the mechanical properties of Si_3N_4 ceramics. The SEM and TEM microstructural analysis of sintered materials show that the applied pressure during the sintering process leads to the orientation of the graphene phase and in consequence causes anisotropy of properties. The differences of friction coefficients were examined with the Ball-on-Disc method for the two directions (parallel and perpendicular to the pressing axis). Also the specific wear rate of the ball for the direction parallel to pressing axis differ significantly in comparison to the wear for the direction perpendicular to the pressing direction.

Keywords: silicon nitride, graphene, Young's modulus, hardness, coefficient of friction, wear rate

1. Introduction

Silicon nitride based ceramics are characterized by a beneficial combination of mechanical, thermal and chemical properties, such as: high bending strength, fracture toughness, abrasion wear resistance, even at elevated temperatures, very good thermal shock resistance and resistance to corrosion. Therefore, silicon nitride is commonly used for the production of cutting

tools, bearing balls, elements of valves and various parts of devices designed to work in hard conditions (temperature, friction, aggressive environment, etc.) [1–3]. Due to high covalent bonding and very low diffusivity of the silicon nitride, densification can only be achieved by applying pressure and/or by introducing sintering aids, typically metal oxides such as MgO , Al_2O_3 , Y_2O_3 , or ZrO_2 . The additives promote a liquid phase formation which provides faster mass transport and leads to consolidation of powder particles to form a dense body. During rapid cooling following the sintering process of the silicon nitride materials a microstructure of Si_3N_4 grains with intergranular glass phase is formed [4]. If Y_2O_3 is the sintering aid, a portion of this glass can be devitrified by heat treating and slow cooling to create crystalline yttrium – aluminum garnet (YAG) [5]. The addition of dispersed phases of metal carbides, nitrides and borides (TiC , TiN , SiC , TiB_2) to Si_3N_4 results in an increase in hardness, fracture toughness and wear resistance of the composite [6–8]. Other benefits from the addition of a dispersed second phase to silicon nitride can be the lowering of the friction coefficient or achieving electroconductivity in this material [9]. Recently, carbon 1D and 2D nanostructures such as nanotubes or graphene have been intensively researched. Graphene, a two-dimensional, crystalline allotrope of carbon is characterized by exceptional electrical, thermal and mechanical properties [10]. Last year, many papers indicated the possibility of using graphene nanoplatelets (GPLs) as filler for ceramic composites [11–13]. Most of the investigated ceramics toughened by the addition of graphene have been obtained by the Spark Plasma Sintering (SPS) method. SPS allows high heating rates and short sintering time together with relatively low sintering temperatures. The toughening enhancement resulting from introducing the graphene nanoplatelets to Si_3N_4

matrix can be greater than 200% [14]. Seiner et al. [15] for the Si_3N_4 composites containing up to 18 wt. % of GPLs have shown anisotropic behavior regarding elastic constants, with symmetry axis defined by the SPS loading direction. This anisotropy was enhanced when fillers were fully contacted. Elastic moduli decreased with an increase of the GPLs content. Other papers have shown also strong anisotropization of thermal and electrical conductivity of nitride ceramics caused by the addition of GPLs [16,17].

The aim of the presented work was to investigate the influence of GPLs addition on selected mechanical and tribological properties of Si_3N_4 based ceramics sintered by the SPS method.

2. Materials and methods

The composites were prepared from the mixture of silicon nitride powder (Si_3N_4 , $\alpha > 90\%$, grade M11, 0.6 μm , H.C. Starck) with the addition of 2 wt. % MgO nanopowder (Inframat) and 2 wt. % 3YTZ (3 mol. % yttria stabilized tetragonal zirconia, $< 0.5 \mu\text{m}$, H.C. Starck). Multilayer graphene nanoplatelets having thickness of 4 nm, referred as GPLs(4) (Cheap Tubes USA graphene nanopowder, 4 nm flakes, purity 99%, average flake thickness $< 4 \text{ nm}$, average lateral particle size 1–2 μm , specific surface area $> 700 \text{ m}^2/\text{g}$), were used as filler for silicon nitride based composites. SEM micrographs of graphene nanoplatelets used in the experiment are presented in Figure 1.

The mixtures, containing 0, 0.5, 1 and 2 wt. % of GPLs(4) were homogenized using Fritsch Pulverisette 6 planetary mill equipped with Si_3N_4 grinding vessel with 5 mm balls. Powders were milled in isopropanol with rotation speed 200 rpm for 8 h. The composites were sintered using Spark Plasma Sintering – SPS (FCT system, Germany) in the temperature range of 1250–1750°C for 5 min and then applied 35 MPa of uniaxial pressure during the whole cycle. Sintered specimens were

disk-shaped with dimensions of 20 mm in diameter and $\sim 5 \text{ mm}$ in thickness.

Microstructure of the materials were studied with an optical microscope, scanning electron microscope SEM JEOL JSM-6460LV and transmission electron microscope TEM TECNAI G2 F20 (200 kV). For TEM analysis, thin foils were prepared using focused ion beam (Quanta 3D System). Density of the sintered samples was measured by the hydrostatic method and their theoretical density calculated by the rule of mixtures, assuming densities of 3.2 g/cm^3 for Si_3N_4 , 6.0 g/cm^3 for 3YTZ, 3.58 g/cm^3 for MgO, and 2.2 g/cm^3 for GPLs. Young's modulus of composites was measured based on the velocity of the ultrasonic waves transition through the sample using the ultrasonic flaw detector Panametrics Epoch III. The hardness and the fracture toughness were determined by the Vickers method under a load of 9.81 and 98.1 N, using a Future Tech FLC-50VX Vickers hardness tester. The stress intensity factor K_{Ic} was calculated from the length of cracks which developed during a Vickers indentation test.

In the Ball-On-Disc tests, the coefficient of friction (COF) and the specific wear rate (Ws) of the sintered samples in contact with Si_3N_4 ball were determined using a CETR UMT-2MT (USA) universal mechanical tester. In the Ball-On-Disc method, sliding contact is brought about by pushing a ball specimen onto a rotating disc specimen under a constant load. The samples had surface flatness and parallelism within 0.02 mm. The roughness of the tested surface was no more than 0.1 μm Ra. The following test conditions were established: ball diameter – 2 mm, applied load – 4 N, sliding speed – 0.1 m/s, diameter of the sliding circle – 3 mm, sliding distance – 1000 m, calculated duration of the test – 10,000 s. The tests were carried out without lubricant at room temperature. After completing the test, according to ISO 20808:2004 E standard, the cross-sectional profile of the wear track at four areas at intervals of 90° was measured using a contact stylus profilometer. Then the average cross-sectional area of

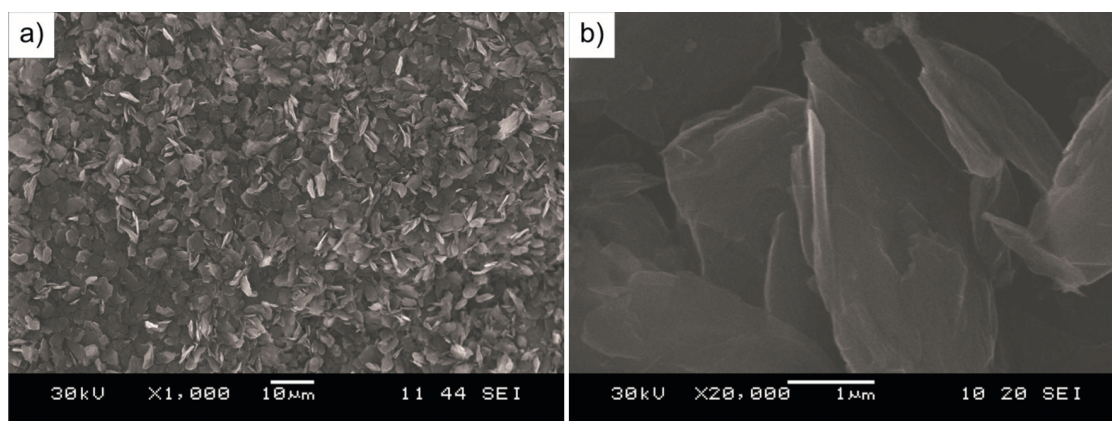


Fig. 1. SEM micrographs of graphene nanoplatelets GPLs(4) used as fillers for Si_3N_4 -matrices: low magnification (a) and high magnification (b)

the wear track was calculated. The volume of material removed was calculated as a product of cross-sectional area of the wear track and their circumference.

3. Results and discussion

Initially, the optimization of sintering temperature for SPS method was carried out to achieve the highest possible density and Young's modulus of the materials. Density and Young's modulus of Si₃N₄ samples containing 1 wt. % of GPLs(4), sintered at temperatures from 1250°C to 1750°C for 5 min and applied pressure of 35 MPa, are presented in Figure 2.

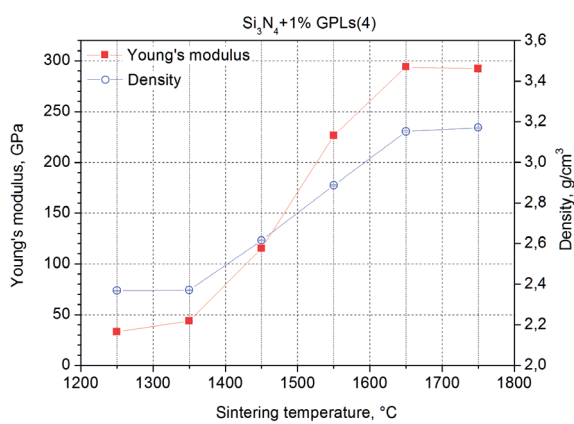


Fig. 2. Density and Young's modulus of Si₃N₄ + 1% GPLs(4) materials sintered at temperatures from 1250°C to 1750°C

The sinterability region for Si₃N₄ + 1% GPLs(4) materials starts at 1650°C (when the sintering pressure and duration are 35 MPa and 5 min respectively). Basing on data presented in Figure 2 the temperature of 1650°C was selected for sintering of all the materials intended for further studies. The studies of mechanical properties (Young's modulus, hardness, fracture toughness, coefficient of friction and wear resistance) for samples

containing 2% of GPLs(4) were made on the planes perpendicular (⊥) and parallel (||) to the pressing axis in SPS sintering process in order to determine the influence of the force direction on properties of the composite. Physical and mechanical properties of silicon nitride based ceramics with the addition of 0–2 wt. % of graphene platelets, sintered with the SPS method at temperature of 1650°C for 5 min, are presented in Table 1.

Relative density (~98%) and fracture toughness (~5 MPa·m^{1/2}) of Si₃N₄ ceramics have not changed significantly (simply in the range of uncertainty of measurements) when GPLs content was increased from 0 to 2 wt. %, while Young's modulus and Vickers hardness decreased from 320 to 276 GPa and from 18.1 to 15.5 GPa, respectively. There were no significant differences between properties of Si₃N₄ samples containing 2% GPLs, measured on the planes perpendicular (⊥) and parallel (||) to the pressing axis in SPS.

The microstructure of Si₃N₄ ceramics with 2% of graphene platelets was rather homogeneous, nevertheless small agglomerates of GPLs were visible in the optical image (Fig. 3a). This can explain the slight deterioration of mechanical properties. In addition to the agglomerates, in the composite microstructure there were also well dispersed graphene platelets visible in TEM images (Fig. 3b).

The coefficients of friction (COF) and specific wear rates for composites in sliding contact with Si₃N₄ ceramic ball were determined at room temperatures in Ball-on-Disc tests. The results are presented in Figures 4 and 5.

The average value of friction coefficient measured at the steady stay (second half of the test) on the plane perpendicular (T) to pressing direction was about 0.6. For the plane parallel (||) to pressing direction the value of COF was higher but did not exceed 0.7, wherein oscillations for this plane were also higher. Specific wear rates of discs $W_s^{(disc)}$ (sample) for both planes were similar ($9 \cdot 10^{-6}$ mm³/N·m for || plane and $7.6 \cdot 10^{-6}$ mm³/N·m for T plane). Significant differences in wear behaviour had

Table 1. Density, Young's modulus, Vickers hardness and fracture toughness of silicon nitride based composites with addition of 0–2 wt. % GPLs(4)

Material composition, wt. %	Density (relative density), g/cm ³ (%)	Young's modulus, GPa	Vickers hardness		Fracture toughness K_{IC} , MPa·m ^{1/2}
			HV 1 kg, GPa	HV 10 kg, GPa	
Si ₃ N ₄ based ceramics – initial	3.19 ±0.01 (98%)	320 ±7	18.8 ±1.1	18.1 ±0.5	4.9 ±0.3
Si ₃ N ₄ + 0.5%GPLs(4)	3.18 ±0.01 (98%)	309 ±4	19.7 ±0.5	17.8 ±0.1	5.0 ±0.1
Si ₃ N ₄ + 1%GPLs(4)	3.15 ±0.01 (98%)	294 ±2	19.4 ±0.5	17.2 ±0.5	4.7 ±0.2
Si ₃ N ₄ + 2%GPLs(4) ⊥	3.16 ±0.01 (98%)	272 ±3	17,9 ±0.6	15.2 ±0.3	4.9 ±0.2
Si ₃ N ₄ + 2%GPLs(4)	–	276 ±3	17,6 ±1.3	15.5 ±0.2	4.8 ±0.2

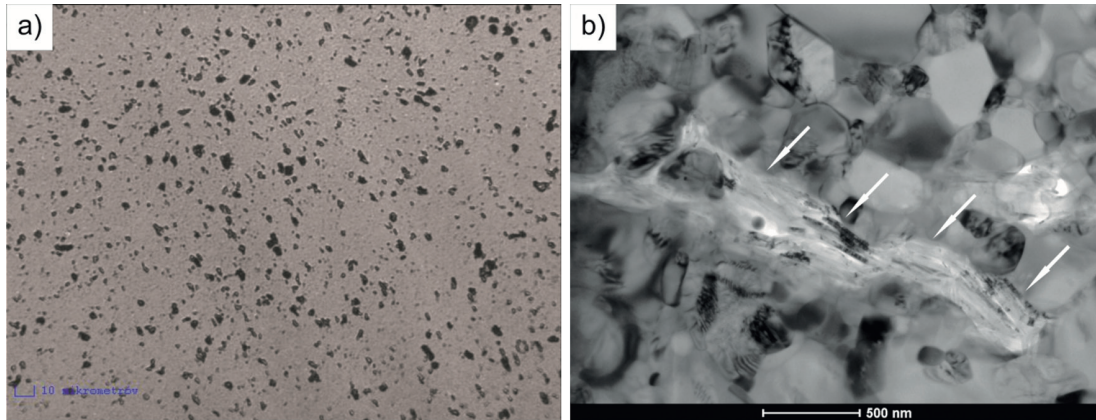


Fig. 3. Microstructures of Si_3N_4 base ceramics with addition 2 wt. % of GPLs(4): optical microscope (a), TEM (b)

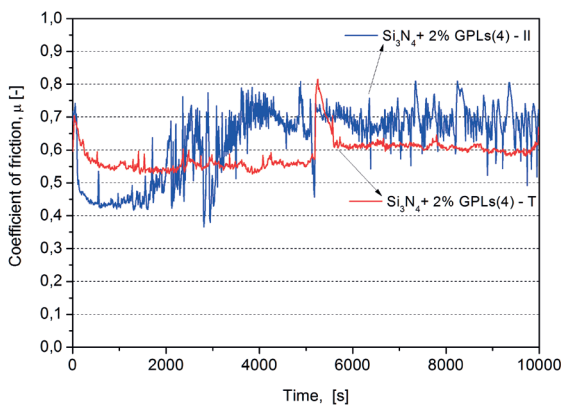


Fig. 4. Friction coefficient of the sample containing 2 wt. % of GPLs(4) for tests carried out on the surface parallel and perpendicular to the pressing direction

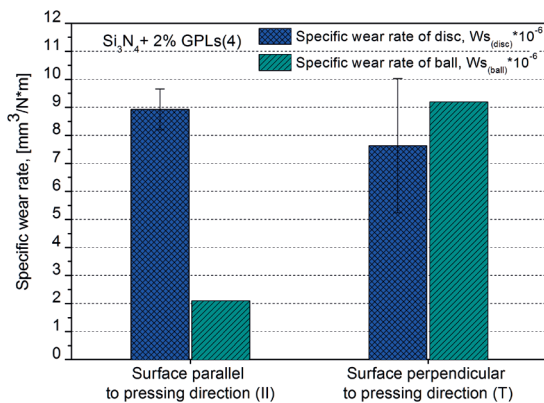


Fig. 5. Ball and disc specific wear rates of the Si_3N_4 sinters containing 2 wt. % of GPLs(4) for tests carried out on the surface parallel and perpendicular to the pressing direction

occurred for the ball. The specific wear rates for ball $W_{s(ball)}$ were $2 \cdot 10^{-6}$ mm³/N·m and $9 \cdot 10^{-6}$ mm³/N·m for II and T plane respectively. One of the possible explanations for this difference in wear rate of ball dependency on the sample surface (II or T) is the preferred orientation

of GPLs caused by pressure during the SPS process. However, further studies are needed to fully explain this phenomenon.

4. Conclusions

Silicon nitride based materials were prepared with different amounts of multilayer graphene nanoplatelets (0–2 wt. %). Relative density and fracture toughness of material were 98% and 5 MPa·m^{1/2} respectively and did not change significantly with GPLs content. The Young's modulus and hardness decreased slightly as a result of graphene addition. Small agglomerates of graphene were visible in the microstructure of Si_3N_4 + 2% GPLs ceramic material, which can explain the slight deterioration of its mechanical properties. There were no significant differences in physical and mechanical properties of Si_3N_4 samples containing 2% GPLs, measured on the planes perpendicular (⊥) and parallel (||) to the SPS pressing axis. An exception was the specific wear rate of the ball mated with Si_3N_4 + 2% GPLs sample. The direction parallel to pressing axis $W_{s(ball)}$ was much smaller in comparison to $W_{s(ball)}$ for the direction perpendicular to the pressing direction. This phenomenon can be explained by the anisotropy of GPLs orientation but further experiments are needed to achieve the required level of confidence.

Acknowledgements

This work was supported within the framework of the statutory activity of The Institute of Advanced Manufacturing Technology, Krakow, Poland (Statutory work No. DS-17.3.3).

This study was carried out within the framework of GRAF-TECH programme, supporting scientific research on the unique graphene characteristics, funded by the Polish National Centre for Research and Development; the project: "Ceramic-graphene composites for cutting tools

and devices parts with unique properties – CERGRAF” (project number: GRAF-TECH/NCBR/03/05/2012).

References

1. Klemm H. 2010. “Silicon nitride for high-temperature applications”. *Journal of the American Ceramic Society* 93 (6) : 1501–1522. DOI: 10.1111/j.1551-2916.2010.03839.x.
2. Ariff T.F., N.S. Shafie, Z.M. Zahir. 2013. “Wear analysis of silicon nitride (Si₃N₄) cutting tool in dry machining of T6061 aluminium alloy”. *Materials, Mechanical Engineering and Manufacture* 268 : 563–567. DOI: 10.4028/www.scientific.net/AMM.268-270.563.
3. Hampshire S. 2007. “Silicon nitride ceramics – review of structure, processing and properties”. *Journal of Achievements in Materials and Manufacturing Engineering* 24 (1) : 43–50.
4. Lange F.F. 2006. “The sophistication of ceramic science through silicon nitride studies”. *Journal of the Ceramic Society of Japan* 114 (11) : 873–879.
5. Korb G., F.I. Bulic, P. Sajgalik, Z. Lences. 2001. Gradient structures in SiAlON’s for improved cutting performance. In G. Kneringer, P. Roedhammer, H. Wildner (Eds.), *Powder Metallurgical High Performance Materials, Vol. 4: Late Papers, Proceedings of the 15th International Plansee Seminar*, 386–396. Reutte: Plansee Holding AG. Retrieved from: http://www.iaea.org/inis/collection/NCLCollectionStore/_Public/33/060/33060919.pdf.
6. Lee C.H., H.H. Lu, C.A. Wang, P.K. Nayak, J.L. Huang. 2010. “Microstructure and mechanical properties of TiN/Si₃N₄ nanocomposites by spark plasma sintering (SPS)”. *Journal of Alloys and Compounds* 508 (2) : 540–545. DOI: 10.1016/j.jallcom.2010.08.116.
7. Blugan G., M. Hadad, T. Graule, J. Kuebler. 2014. “Si₃N₄–TiN–SiC three particle phase composites for wear applications”. *Ceramics International* 40 (1 Part B) : 1439–1446. DOI: 10.1016/j.ceramint.2013.07.027.
8. Klimczyk P. 2011. SiC-based composites sintered with high pressure method. In M. Mukherjee (Ed.), *Silicon Carbide – Materials, Processing and Applications in Electronic Devices*, 309–334. InTech. DOI: 10.5772/852.
9. Putyra P., J. Laszkiewicz-Lukasik, P. Wyzga, M. Podsiadlo, B. Smuk. 2011. “The selection of phase composition of silicon nitride ceramics for shaping with the use of EDM machining”. *Journal of Achievements in Materials and Manufacturing Engineering* 48 (1) : 35–40.
10. Geim A.K., K.S. Novoselov. 2007. “The rise of graphene”. *Nature Materials* 6 (3) : 183–191. Retrieved from: <http://dx.doi.org/10.1038/nmat1849>.
11. Kim H.J., S.-M. Lee, Y.-S. Oh, Y.-H. Yang, Y.S. Lim, D.H. Yoon, C. Lee, J.Y. Kim, R.S. Ruoff. 2014. “Unoxidized graphene/alumina nanocomposite: fracture- and wear-resistance effects of graphene on alumina matrix”. *Nature Scientific Reports* 4 : 5176. DOI: 10.1038/srep05176.
12. Ramirez C., P. Miranzo, M. Belmonte, M.I. Osendi, P. Poza, S.M. Vega-Diaz, M. Terrones. 2014. “Extraordinary toughening enhancement and flexural strength in Si₃N₄ composites using graphene sheets”. *Journal of the European Ceramic Society* 34 (2) : 161–169. DOI: 10.1016/j.jeurceramsoc.2013.08.039.
13. Kvetková L., A. Duszová, P. Hvizdoš, J. Dusza, P. Kun, C. Balázsi. 2012. “Fracture toughness and toughening mechanisms in graphene platelet reinforced Si₃N₄ composites”. *Scripta Materialia* 66 (10) : 793–796. DOI: 10.1016/j.scriptamat.2012.02.009.
14. Walker L.S., V.R. Marotto, M.A. Rafiee, N. Koratkar, E.L. Corral. 2011. “Toughening in graphene ceramic composites”. *ACS Nano* 5 (4) : 3182–3190. DOI: 10.1021/nn200319d.
15. Seiner H., C. Ramirez, M. Koller, P. Sedláč, M. Landa, P. Miranzo, M. Belmonte, M.I. Osendi. 2015. “Elastic properties of silicon nitride ceramics reinforced with graphene nanofillers”. *Materials & Design* 87 : 675–680. DOI: 10.1016/j.matdes.2015.08.044.
16. Miranzo P., E. García, C. Ramírez, J. González-Julián, M. Belmonte, M.I. Osendi. 2012. “Anisotropic thermal conductivity of silicon nitride ceramics containing carbon nanostructures”. *Journal of the European Ceramic Society* 32 (8) : 1847–1854. DOI: 10.1016/j.jeurceramsoc.2012.01.026.
17. Ramirez C., L. Garzón, P. Miranzo, M.I. Osendi, C. Ocal. 2011. “Electrical conductivity maps in graphene nanoplatelet/silicon nitride composites using conducting scanning force microscopy”. *Carbon* 49 (12) : 3873–3880. DOI: 10.1016/j.carbon.2011.05.025.

